hep-ph 1203.5416

arXiv:1203.5416v2 [hep-ph] 3 Jul 2012

CERN-PH-EP-2012-064, DESY-12-039

Evaluation of the Strong Coupling Constant α_s Using the ATLAS Inclusive Jet Cross-Section Data

B. Malaescu[1] and P. Starovoitov[2]

[1]*CERN, CH–1211, Geneva 23, Switzerland*
[2]*DESY, 22607, Notkestraße 85, Hamburg, Germany*

(Dated: July 4, 2012)

We perform a determination of the strong coupling constant using the latest ATLAS inclusive jet cross section data, from proton-proton collisions at $\sqrt{s}$ = 7TeV, and their full information on the bin-to-bin correlations. Several procedures for combining the statistical information from the different data inputs are studied and compared. The theoretical prediction is obtained using NLO QCD, and it also includes non-perturbative corrections. Our determination uses inputs with transverse momenta between 45 and 600 GeV, the running of the strong coupling being also tested in this range. Good agreement is observed when comparing our result with the world average at the Z-boson scale, as well as with the most recent results from the Tevatron.

I. INTRODUCTION

The strong coupling constant α_s is one of the fundamental parameters of the Standard Model of particle physics (SM). Testing the energy dependence (running) of α_s over a wide range provides an implicit test of QCD and probes potential effects from "New Physics".

In this paper we present a determination of α_s exploiting the recently published ATLAS inclusive jet cross section data [1], allowing for the first test of the running of α_s up to the TeV scale. The only other input based on experimental measurements consists of the NLO QCD proton parton density functions (PDFs), as obtained by various groups from other independent data sets. These PDFs allow us to compute, for a given α_s value, the perturbative NLO QCD prediction of the inclusive jet cross section, which is then corrected for non-perturbative effects. Our evaluation procedure goes through the determination of $\alpha_s(M_Z^2)$ using the measured cross section in each data bin, followed by the propagation of the experimental uncertainties and bin-to-bin correlations. Finally, an unbiased averaging procedure is used and the uncertainties are propagated to the corresponding result.

In Sec. II we discuss the information provided by the ATLAS inclusive jet cross section data, while in Sec. III we describe the theoretical prediction used in the α_s determination. Several possible procedures of data treatment are discussed in Sec. IV, while the corresponding results are presented in Sec. V. Our conclusions from this study are discussed in Sec. VI.

II. INPUT DATA

In this study we exploit the unfolded double-differential ATLAS inclusive jet cross section data, in bins of the absolute rapidity ($|y|$) and as a function of the jet transverse momentum ($p_{\rm T}$), together with the statistical and systematic uncertainties, and their correlations [1]. Jets are defined using the anti-k_t jet algorithm [2] implemented in the FASTJET [3] package. This measurement, performed for anti-k_t jets with a distance parameter R=0.4 and R=0.6 respectively, covers a large phase-space region going up to 4.4 in absolute rapidity and from 20 GeV to more than 1 TeV in $p_{\rm T}$. The detailed analysis of the uncertainties and their correlations is one of the important achievements of this measurement.

The dominant uncertainty in this measurement is due to the jet energy scale (JES) calibration. Other smaller systematic uncertainties are due to the luminosity measurement, multiple proton-proton interactions ("pile-up"), trigger efficiency, jet reconstruction and identification, jet energy resolution and deconvolution of detector effects (unfolding). The information on the (anti-) correlations between the various $|y|$ and $p_{\rm T}$ bins is provided for these components, using a set of 87 independent nuisance parameters. These nuisance parameters also provide the information on the asymmetries of these uncertainties (mainly due to the steeply falling $p_{\rm T}$ spectrum). This type of information cannot be incorporated in a covariance matrix. Depending on the rapidity bin, the systematic uncertainties account for $20-60\%$ at low $p_{\rm T}$, and $20-40\%$ at high $p_{\rm T}$, while they are smaller for intermediate jet transverse momentum values.

The statistical uncertainties and their (anti-) correlations are provided through a covariance matrix for each rapidity bin. Here the correlations are due to the transfers of jets between the different $p_{\rm T}$ bins (performed in the unfolding), as well as to the fact that several jets going into the spectrum can be produced in the same event. The statistical uncertainties are in general much smaller than the systematics, except for the high $p_{\rm T}$ region, where they can be larger.

It has been pointed out in [1] that, when performing the comparison between data and the theoretical prediction, somewhat larger differences are observed for R=0.4 than for R=0.6 jets. However, the χ^2/dof, computed taking into account the correlations, is reasonable in both cases. In our study, we do not perform a simultaneous treatment of the two jet sizes, because the correlations of the uncertainties of these measurements (expected to

be large) are not available. We use the measurement of jets with R=0.6 for determining our nominal result, while the comparison with the result using jets with R=0.4 provides a systematic uncertainty.

III. THEORETICAL PREDICTION

Theoretical predictions for the inclusive jet cross sections are calculated in perturbative QCD at next-to-leading order (NLO) using the NLOJET++ [4] program, while the effects of hadronisation and underlying event activity on jet production have been studied using Monte Carlo generators. Each bin of the perturbative cross section is multiplied by the non-perturbative corrections to obtain the prediction at the particle level that can be compared to the data.

A. Perturbative QCD calculations

The inclusive jet cross section is calculated using the CT10 [5] NLO parton density functions. The p_{T} and rapidity binnings follow the one from ATLAS inclusive jet cross section measurement [1]. For the sake of simplicity, the renormalisation μ_{R} and the factorisation μ_{F} scales for the central result are set to be the same in the calculation

$$\mu = \mu_{\mathrm{R}} = \mu_{\mathrm{F}} = p_{\mathrm{T}}^{\mathrm{max}},$$

where $p_{\mathrm{T}}^{\mathrm{max}}$ is the transverse momentum of the leading jet in a given rapidity bin.

To allow for fast and flexible evaluation of the cross section using different values of α_S, as well as for evaluation of the PDF and scale uncertainties, the APPLGRID [6] software was interfaced with NLOJET++ in order to calculate the perturbative coefficients once and store them in a look-up table.

B. PDF inputs

There are several PDF fitter groups who provide alternative PDF sets using slightly different theoretical approaches and various experimental data from different scattering processes as input. Usually PDF groups provide the central (best-fit, given an $\alpha_s(M_Z^2)$ value) PDF set together with a collection of uncertainty PDF sets. The central set is used for the theory prediction, while the uncertainty sets are needed for the evaluation of the PDF uncertainties in the calculation.

The best-fit CT10 PDF set is obtained with $\alpha_s(M_Z^2) = 0.118$. In order to facilitate the studies of the dependence of observables upon the strong coupling CT10 PDF is provided with the special list of PDF sets, obtained by scanning the $\alpha_s(M_Z^2)$. The PDF sets in this list were refitted while the $\alpha_s(M_Z^2)$ was varied in the $[0.113, 0.123]$ range in steps of 0.001.

TABLE I: The range of α_S-scan and the best-fit $\alpha_S(M_Z^2)$ values for PDF sets used in the analysis.

PDF set	$\alpha_S(M_Z^2)^{\mathrm{best}}$	$\alpha_S(M_Z^2)^{\mathrm{min}}$	$\alpha_S(M_Z^2)^{\mathrm{max}}$	step
CT10	0.118	0.113	0.123	0.001
MSTW 2008	0.1202	0.110	0.130	0.001
HERAPDF 1.5	0.1176	0.114	0.122	0.001
NNPDF 2.1	0.1190	0.110	0.130	0.001

Given the α_S-scan, we have calculated the inclusive jet cross section $\sigma^{Th}(\alpha_S, p_{\mathrm{T}}, |y|)$ for each α_S-point in the scan. Such a function provides a one-to-one correspondence between the $\alpha_S(M_Z^2)$ and the jet cross section values in each $(p_{\mathrm{T}}, |y|)$ bin. For the values of α_S outside the scan range (between scan points) a linear extrapolation (interpolation) is used.

In contrast to CT10, the central MSTW 2008 fit [7] suggests that $\alpha_S(M_Z^2) = 0.1202$ and MSTW group provides the α_S-scan in the range $[0.110, 0.130]$. For the NNPDF 2.1 [8, 9] the central PDF set is fitted with $\alpha_S(M_Z^2)$ fixed to 0.1190 and the scan is performed for α_S values from 0.110 to 0.130 . Finally, for the HERAPDF 1.5 [10] an α_S scan has been performed, from 0.114 to 0.122, with the best-fit value at $\alpha_S(M_Z^2) = 0.1176$. All the PDF sets provide the α_S-scan with the same stepping. The nominal $\alpha_S(M_Z^2)$ values for the various PDF sets, as well as the ranges of the scans, are summarized in table I.

C. Non-perturbative corrections

The fixed-order NLO QCD calculations predict hard parton-level cross sections, which need to be corrected for non-perturbative effects when compared to data. After the hard scattering phase of pp-collision partons emit radiation and evolve down to lower scales. At a very low scale, when strong coupling becomes very large, the non-perturbative phase of collision starts, where coloured partons form colourless real hadrons. This process is called hadronisation. There is also underlying event (UE) activity, which happens in parallel to the hard scattering. The UE consists of interactions of beam remnants as well as from multiple parton interactions.

The hadronisation process leads to a decrease of the jet p_{T}, while the UE adds extra particles to the jet and results in an increase of jet transverse momentum. The effects of both hadronisation and UE are most pronounced at low p_{T}. Since the effect of UE on the jet p_{T} increases with increasing size of the jet (jet radius R) while the effect of the hadronisation process decreases, if the jet radius grows, two separate sets of corrections and uncertainties were derived for jets with $R = 0.4$ and $R = 0.6$. The R dependence of the contributions of non-perturbative effects to the jet transverse momentum was calculated in [11, 12]. It has been shown that the hadronisation contribution is proportional to $-1/R$, while the

TABLE II: Set of tunes used for the different generators.

Generator	Tune
PYTHIA 6.425	AUET2B LO**
	AUET2 LO** AMBT1
	AMBT2B CTEQ6L1
	Perugia 2010
	Perugia 2011
PYTHIA 8.150	4*C*
HERWIG++ 2.5.1	UE7000-2

UE contribution varies as R^2. The leading R dependence was found to be quite similar for all jet algorithms. For $R = 0.4$, the correction factors are dominated by the effect of hadronisation and are approximately 0.95 at jet $p_{\mathrm{T}} = 20$ GeV, increasing closer to unity at higher p_{T}. For $R = 0.6$ the correction factors are dominated by the UE and are approximately 1.6 at jet $p_{\mathrm{T}} = 20$ GeV decreasing to between $1.0 - 1.1$ for jets above $p_{\mathrm{T}} = 100$ GeV.

The non-perturbative corrections are evaluated using leading-logarithmic parton shower generators. The corrections are derived using PYTHIA 6.425 with the ATLAS AUET2B CTEQ6L1 tune [13]. These are evaluated as the bin-wise ratio of cross section calculated after hadronisation and with simulation of the underlying event activity, to the one at parton-level and without underlying event. The parton-level cross section in each bin is then multiplied by the corresponding correction:

$$\frac{d^2\sigma^{particle}}{dp_T^{jet}d|y|} = \frac{d^2\sigma^{NLO\ QCD}}{dp_T^{jet}d|y|} \times \delta^{non-pert}\left(p_T^{jet}, |y|\right). \quad (1)$$

The uncertainty of the non-perturbative corrections is estimated as the maximum spread of the correction factors obtained from PYTHIA 6.425 using the AUET2B LO**, AUET2 LO**, AMBT2B CTEQ6L1, AMBT1, Perugia 2010, and Perugia 2011 tunes (PYTUNE_350), and the PYTHIA 8.150 tune 4*C* [13–16], as well as the corrections obtained from HERWIG++ 2.5.1 [17] using the UE7000-2 [13] tune (see table II). In our analysis we have used the non-perturbative corrections evaluated in [1].

We would like to mention that an analytic estimate for the non-perturbative correction to the inclusive jet spectrum was proposed [11]. It was used in [18] to compare the perturbative QCD calculations to the first ATLAS inclusive jet measurement [19]. The values for analytic and MC-based corrections were found to be compatible [18]. It would be very interesting to include the analytic evaluation of non-perturbative effects in the α_s determination, once the flavour decomposition of inclusive jet spectra and UE parameters are measured experimentally.

IV. α_S EVALUATION PROCEDURE

In this section we describe several possible procedures for determining $\alpha_S(M_Z^2)$ from the inclusive jet cross section data. First we explain how we exploit the experimental information in individual (p_{T}; $|y|$) bins, together with the propagation of the uncertainties and bin-to-bin correlations. Then we discuss several possible averaging procedures, for combining the statistical information of the various (p_{T}; $|y|$) bins, in order to obtain an average $\alpha_S(M_Z^2)$ value. We also discuss the specific properties of these various procedures.

A. Determination of α_S in individual (p_{T}; $|y|$) bins

An α_S value is obtained in each bin of the measurement, using the theoretical prediction and the experimental cross section. The theoretical prediction provides, in each (p_{T}; $|y|$) bin, a one-to-one mapping between α_S and the inclusive jet cross section (see previous section). The nominal value of the measured cross section is mapped by this procedure to the nominal α_S value in the corresponding bin. All the experimental uncertainties of cross sections, together with their bin-to-bin correlations, are propagated to the determined α_S values, using pseudo-experiments (toys), as explained in the following subsection.

B. Propagation of data uncertainties and correlations

A series of pseudo-experiments, each of them including a complete set of cross section values in all the (p_{T}; $|y|$) bins, are generated using the experimental input described in section II.

The statistical fluctuations are generated using the information provided in the published covariance matrices. Each matrix is diagonalised, and a set of independent random numbers (Gaussian distributions with widths given by the eigenvalues) is generated in the corresponding space. The unitary matrices of eigenvectors are then used to propagate this set of random values to the physical space of the (p_{T}; $|y|$) bins.

Each nuisance parameter for a given component of the systematic uncertainties is treated as 100% correlated between all the bins. The various nuisance parameters are treated as independent with respect to each other. The distributions of the experimental uncertainties are modelled using asymmetric Gaussian shapes, centered at zero, with 50% probability of generating pseudo-measurements at negative or positive values. The two widths of the asymmetric Gaussian are equal to the corresponding un-

certainties [1]. In a given pseudo-experiment, the contributions of all the fluctuated nuisance parameters are added linearly to the nominal measured value. After adding the contribution of the statistical uncertainty, the value of the pseudo-measurement is obtained.

For each pseudo-experiment, the same procedure as for the nominal measurements is applied to obtain an α_S value in each bin. This allows the propagation of all the experimental uncertainties, with their correlations and their asymmetric distributions, from the cross section level to the α_S values.

In view of the study of various possible averaging procedures, it is interesting to determine an approximate (after the symmetrisation of uncertainties) covariance matrix of the α_S values. The effect of the needed symmetrisation is rather small at this level, due to a partial compensation between the asymmetries of the cross section uncertainties and the non-linear effects in the theoretical prediction (for $\sigma(\alpha_S)$). It is also interesting to determine a covariance matrix of the cross section measurements; however, the effect of the symmetrisation is larger at that level.

C. Averaging procedures

In order to study and avoid potential biases introduced by some averaging procedures, several options for performing the combination of the inputs in the various (p_{T}; $|y|$) bins have been tested here. All of them aim at obtaining an average value of the strong coupling constant (α_S^{Av}).

1. *Simple average*

The first procedure consists of a simple average, where all the input α_S values have the same weight (equal to the inverse of the number of inputs). Although the final uncertainty on this average might not be optimal, the weights of the input α_S values are well behaved (i.e. they are all in the $[0;1]$ interval, with the sum equal to unity).

2. *Weighted average*

The 2^{nd} procedure which has been tested consists of a weighted average, where the weights of the input α_S values are proportional to the inverse of their squared total uncertainties (obtained after symmetrisation). The weights used in this procedure are also well behaved, in the sense defined above. They also have the advantage that more precise contributions get larger weights. A variation of this procedure has also been tested, where the weights are proportional to the inverse of the squared statistical uncertainty. Actually, the statistical uncertainties exhibit much smaller correlations comparing to the systematic ones, motivating this additional test.

3. *Standard χ^2 minimisation*

The 3^{rd} averaging procedure consists of the minimisation of a "standard" χ^2 with correlations

$$\chi^2 = (\bar{\alpha}_S^{\mathrm{Nom}} - \bar{\alpha}_S^{\mathrm{Av}}) \cdot C^{-1} \cdot (\bar{\alpha}_S^{\mathrm{Nom}} - \bar{\alpha}_S^{\mathrm{Av}})^T, \qquad (2)$$

with respect to α_S^{Av}. Here, $\bar{\alpha}_S^{\mathrm{Nom}}$ is the vector of nominal α_S values (obtained in individual (p_{T}; $|y|$) bins) entering the average, C is their covariance matrix, while $\bar{\alpha}_S^{\mathrm{Av}}$ is a vector containing values equal to α_S^{Av} (to be fitted) and having the same size as $\bar{\alpha}_S^{\mathrm{Nom}}$.

It has been shown in [20] that this approach, although very commonly used, can yield biased average values. Actually, in presence of (not very well understood) strong correlations among the inputs, the average value can be even outside the range of the input values, which seems unacceptable. Indeed, the minimisation of the function in Eq. 2, with respect to α_S^{Av} (equivalent to the minimisation of the variance of the output of a weighted average, cf. Gauss-Markov theorem), yields (see for example [21])

$$\alpha_S^{\mathrm{Av}} = \frac{\bar{1} \cdot C^{-1} \cdot (\bar{\alpha}_S^{\mathrm{Nom}})^T}{\bar{1} \cdot C^{-1} \cdot \bar{1}^T}, \qquad (3)$$

where $\bar{1}$ is a vector with all the entries equal to unity and the same size as $\bar{\alpha}_S^{\mathrm{Nom}}$. Just as in the two previous methods, the average resulting from the χ^2 minimisation is a weighted mean of the input values. However, the only constraint on these weights is that their sum equals unity. There is no constraint on the range of the weights and, in presence of strong correlations, these weights can even be negative or larger than unity.

The explanation of the bias in this procedure, as provided in [20], makes responsible the input covariance matrix because of "the linearisation on which the usual error propagation relies". However, two different problems of this approach have been pointed out in [22]. Actually, Eq. 2 involves the inversion of the covariance matrix, which is ill-behaved (a small change in the covariance matrix can have an important impact on its inverse, hence on the weights and the average). Without special techniques, neither the inverse can be computed, nor the minimisation can be performed. Furthermore, this χ^2 definition treats all the uncertainties as absolute (i.e. corresponding to additive effects), whereas at least some of them (like the uncertainty on the luminosity etc.) should be treated as relative uncertainties (i.e. corresponding to multiplicative effects).

[1] This model of the distributions is motivated by the origin of the asymmetric uncertainties, due to the shape of the p_{T} spectra. However, as explained later, other possible models of these distributions have been tested.

4. Modified χ^2 minimisation

A possible solution to these problems of the "standard" χ^2 minimisation has been provided in [20]. It consists in introducing, for each correlated systematic uncertainty, one nuisance parameter in the χ^2 definition, together with one extra constraint term. For a normalisation uncertainty, a scaling factor is applied to both data and the uncorrelated uncertainties. This is equivalent to introducing the corresponding nuisance parameter as a scaling factor on the theoretical prediction. This alternative approach is used for example in [22, 23]. For an absolute uncertainty, the nuisance parameter acts a coherent additive shift of the theoretical prediction. However, it has been shown (see [24, 25]) that, if all the systematic uncertainties correspond to (are treated as) additive effects, the approach using nuisance parameters is equivalent to the one of the "standard" χ^2 with correlations (Eq. 2).

This solution, treating the systematic uncertainties as nuisance parameters in the fit, is commonly known as "profiling". It often leads to reduced systematic uncertainties, as they are constraint by the χ^2 minimisation. However, this reduction strongly relies on the bin-to-bin correlations of the systematic uncertainties, as each nuisance parameter is treated as 100% correlated between the bins. This strong assumption (exploited for propagating statistical information between the different phase-space regions) relies on information that is difficult to check in a particular measurement and is therefore, in most cases, not justified. This yields too optimistic results, as the uncertainties on the shape and correlations for each component of the systematic uncertainties should also be taken into account. It should be pointed out that the same assumptions and uncertainty reductions are implicit in the "standard" χ^2 with correlations (Eq. 2). In order to better understand this problem, one can consider an example where, in the performance studies, a given component of the systematic uncertainty has been conservatively overestimated in some particular phase-space region. This conservative approach would be "exploited" by the fitting procedure, in order to reduce the corresponding component in all the phase-space regions.

In our case, the only systematic uncertainty for which the correlations are perfectly known is the one on the normalisation (i.e. the experimental uncertainty of the ATLAS luminosity). This motivates the fourth combination procedure that we have tested, where the luminosity uncertainty is treated as nuisance parameter in the fit (it is "profiled"), while all the other uncertainties are integrated in a partial covariance matrix. Therefore, the χ^2 definition will include a contribution from the comparison between data and theory, involving this partial covariance matrix, plus a constraint on the luminosity shifts.

As it is straightforward to propagate a luminosity variation to the cross section, the first implementation of this combination procedure uses the χ^2 test defined as

$$\chi^2_{\rm tot}\left(\sigma(\alpha_s);\beta_{\rm L}\right) = \left(\frac{\beta_{\rm L}-1}{\epsilon_{\rm L}}\right)^2 + \left(\bar{\sigma}_s^{\rm Nom} - \bar{\sigma}_s^{\rm Th}(\alpha_s^{\rm Av})\cdot\beta_{\rm L}\right)\cdot C^{-1}_{-{\rm L};\sigma}\cdot\left(\bar{\sigma}_s^{\rm Nom} - \bar{\sigma}_s^{\rm Th}(\alpha_s^{\rm Av})\cdot\beta_{\rm L}\right)^T \quad (4)$$

Here, $\bar{\sigma}_s^{\rm Nom}$ is the vector of nominal experimental cross section values, $\bar{\sigma}_s^{\rm Th}(\alpha_s^{\rm Av})$ is the vector of theoretical cross section values computed for $\alpha_s^{\rm Av}$ (to be fitted), $C_{-{\rm L};\sigma}$ is the covariance matrix of the experimental cross section measurements, including all the uncertainties but the one for the luminosity, $\beta_{\rm L}$ is the luminosity scaling factor (ratio of the scaled to the nominal luminosity), and $\epsilon_{\rm L}$ is the luminosity relative uncertainty. The first contribution to the total χ^2 is given by a term $(\chi^2_{\rm L}(\beta_{\rm L}))$ constraining the shifts of the luminosity nuisance parameter, while the second $(\chi^2_{\rm d}\left(\sigma(\alpha_s);\beta_{\rm L}\right))$ comes from the comparison between data and theory at the cross section level.

As explained in subsection IV B, the determination of the covariance matrix at the cross section level involves a larger symmetrisation, comparing to the determination of the covariance matrix of the α_s values. This motivates a second implementation of this combination procedure, driven by the χ^2 test:

$$\chi^2_{\rm tot}(\alpha_s;\beta_{\rm L}) = \left(\frac{\beta_{\rm L}-1}{\epsilon_{\rm L}}\right)^2 + \left(\bar{\alpha}_s^{\rm Nom} - \bar{\alpha}_s^{\rm Av}\left(\beta_{\rm L}\right)\right)\cdot C^{-1}_{-{\rm L};\alpha_S}\cdot\left(\bar{\alpha}_s^{\rm Nom} - \bar{\alpha}_s^{\rm Av}\left(\beta_{\rm L}\right)\right)^T. \quad (5)$$

It involves the covariance matrix of the α_s values ($C_{-{\rm L};\alpha_S}$, including all the uncertainties except the one for the luminosity), which is better defined, as explained above. $\bar{\alpha}_s^{\rm Av}\left(\beta_{\rm L}\right)$ is a vector containing values equal to $\alpha_s^{\rm Av}\left(\beta_{\rm L}\right)$ (the same for all the $(p_{\rm T};\,|y|)$ bins) and having the same size as $\bar{\alpha}_s^{\rm Nom}$. Here we have again the first contribution given by the term constraining the shifts of the luminosity nuisance parameter, while the second $(\chi^2_{\rm d}\left(\alpha_s;\beta_{\rm L}\right))$ comes from the comparison between data and theory, at the α_s level. However, as the theoretical predictions of the cross section values in the various $(p_{\rm T};\,|y|)$ bins exhibit slightly different α_s dependencies (due to NLO QCD and non-perturbative effects), the analytical dependence of $\alpha_s^{\rm Av}$ on a luminosity shift can be only approximate. In this second implementation, we use the following ansatz:

$$\alpha_s^{\rm Av}\left(\beta_{\rm L}\right) \approx \alpha_s \times \left(1 + \frac{\beta_{\rm L}-1}{1.8}\right), \quad (6)$$

which is motivated by the small size of the non-linear effects in the theoretical prediction, together with an empirical observation, as explained in section V E below.

5. Geometrical average

The first three combination procedures described above, make use of weighted averages. They distinguish

between each other by the way how the weights of the inputs in the average are obtained. Another (the fifth) possibility that we have considered for performing the combination consists in a geometrical average:

$$\alpha_S^{\rm Av} = \left(\prod_{i=1}^{n} \alpha_S^{\rm Nom,i} \right)^{\frac{1}{n}}, \qquad (7)$$

where $\alpha_S^{\rm Nom,i}$ runs over the n inputs of the combination.

V. EXPERIMENTAL RESULTS

In this section we present the results for the α_S determinations in the individual ($p_{\rm T}$; $|y|$) bins, using anti-k_t jets with R=0.6, followed by the results of the various combination procedures. We also discuss the issue of the disagreement between the results obtained for anti-k_t jets with R=0.4 and R=0.6, respectively.

A. Individual ($p_{\rm T}$; $|y|$) bins and their correlations

Following the prescription described in section IV A, a nominal α_S value has been determined in each ($p_{\rm T}$; $|y|$) bin, while the statistical and systematic uncertainties, together with their correlations, have been propagated using pseudo-experiments. Fig. 1 shows a few examples of $\alpha_S(M_Z^2)$ distributions, as obtained from 10^6 pseudo-experiments, in the central $|y|$ region, in four different $p_{\rm T}$ bins. Some asymmetries can be seen in these distributions. They are due to the asymmetries in the data uncertainties and to the non-linear dependence of the theoretical cross sections on α_S (from the theoretical calculation and its extrapolation to low and large α_S values, outside the region where the α_S scan is available).

For very low and very large $p_{\rm T}$ values, the total data uncertainties are relatively large. This is mainly due to the JES uncertainty, while the statistical uncertainties are also large at high $p_{\rm T}$. In these regions of the $p_{\rm T}$ spectra, a fluctuation of the cross section by $\pm 1\sigma$ (or more) yields α_S values for which the theoretical prediction is not reliable. Actually, the PDF determinations are not reliable for the corresponding large or low α_S values, while the perturbative calculations also exhibit problems at large α_S. It is for this reason that we discard the $p_{\rm T}$ bins with large experimental uncertainties in the final α_S average computation, and we estimate a systematic uncertainty due to this choice. Because of their large uncertainties, these bins would in any case have a small impact on the average, therefore the estimated uncertainty associated to dropping these bins is small. A number of 42 ($p_{\rm T}$; $|y|$) bins are used in the computation of the various averages. The corresponding ($[p_{\rm T}^{\rm min}; p_{\rm T}^{\rm max}]$; $[|y|_{\rm min}; |y|_{\rm max}]$) ranges, as well as the labels/numbers used for these bins, are given in table III.

TABLE III: $p_{\rm T}$ ranges ($[p_{\rm T}^{\rm min}; p_{\rm T}^{\rm max}]$) used for the α_S determination in various $|y|$ intervals ($[|y|_{\rm min}; |y|_{\rm max}]$). The third column indicates the label used for the $|y|$ bins, while the last column gives the range of numbers assigned to the corresponding ($p_{\rm T}$; $|y|$) bins (ordered in increasing $p_{\rm T}$ and $|y|$).

$[\|y\|_{\rm min}; \|y\|_{\rm max}]$	$[p_{\rm T}^{\rm min}; p_{\rm T}^{\rm max}]$(GeV)	$\|y\|$ bin label	bin numbers
$[0; 0.3]$	[45;600]	$\|y\|_1$	1-10
$[0.3; 0.8]$	[45;600]	$\|y\|_2$	11-20
$[0.8; 1.2]$	[45;500]	$\|y\|_3$	21-29
$[1.2; 2.1]$	[45;310]	$\|y\|_4$	30-36
$[2.1; 2.8]$	[60;210]	$\|y\|_5$	37-40
$[2.8; 3.6]$	[80;110]	$\|y\|_6$	41
$[3.6; 4.4]$	[80;110]	$\|y\|_7$	42

The same sets of pseudo-experiments have been used to determine the (total) covariance and correlation matrices, for the cross sections and α_S values respectively (see Fig. 2), in the ($p_{\rm T}$; $|y|$) bins used for the final combination. Although, as explained above, a slightly larger symmetrisation is needed in order to compute these matrices at the cross section level, it is interesting to remark that the correlation matrices at the α_S and cross section level are very similar.

B. Results with a simple average

The combination using a simple average (SA) of all the input α_S values yields

$$\alpha_S^{\rm SA} = 0.1149^{+0.0047}_{-0.0048},$$

where the quoted uncertainty is experimental only. These uncertainties are obtained by computing (from the pseudo-experiments) the variances of the positive and, respectively, negative fluctuations with respect to the nominal value. These uncertainties are rather symmetric, although the asymmetries are slightly larger when computing the values in individual ($p_{\rm T}$; $|y|$) bins, or even the simple averages of the $p_{\rm T}$ bins in some particular $|y|$ bin.

C. Results with a weighted average

While in the previous combination method the same weight was assigned to all the input α_S values, here we benefit more from precise measurements, using weights proportional to the inverse of the squared total uncertainty. However, the gain in precision is not very big, because the various measurements that are used have rather similar precisions. Actually, all the corresponding weights are in the range between 0 and 1, the ratio of the largest to the smallest weight being ≈ 2.5.

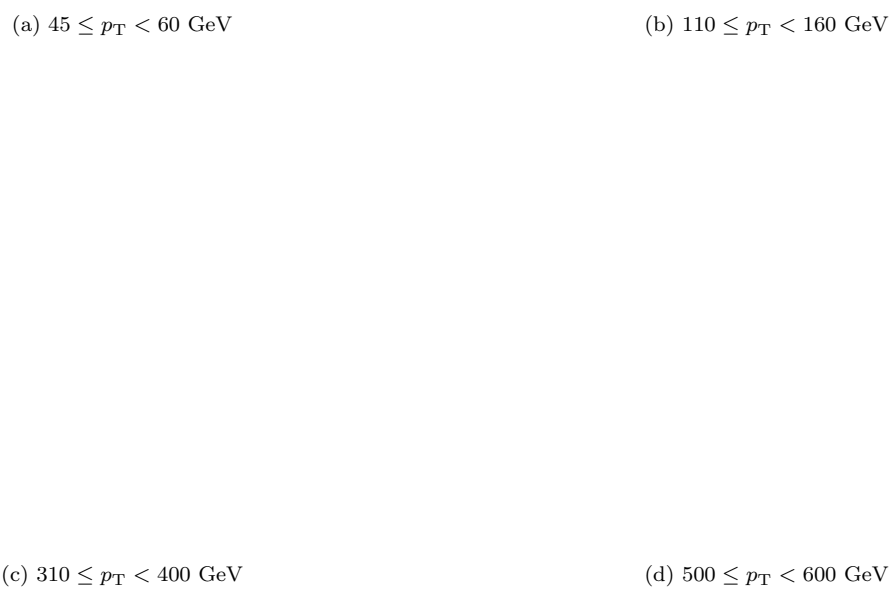

(a) $45 \leq p_{\mathrm{T}} < 60$ GeV

(b) $110 \leq p_{\mathrm{T}} < 160$ GeV

(c) $310 \leq p_{\mathrm{T}} < 400$ GeV

(d) $500 \leq p_{\mathrm{T}} < 600$ GeV

FIG. 1: Examples of distributions of $\alpha_S(M_Z^2)$, as obtained from 10^6 pseudo-experiments, for anti-k_t jets with R=0.6, in the central rapidity region ($0 \leq |y| < 0.3$), in several p_{T} bins.

Computing this weighted average (WA) in the individual $|y|$ intervals given in table III, we obtain

$$\begin{aligned}
\alpha_S^{\mathrm{WA}}(|y|_1) &= 0.1155^{+0.0067}_{-0.0069},\\
\alpha_S^{\mathrm{WA}}(|y|_2) &= 0.1167^{+0.0073}_{-0.0077},\\
\alpha_S^{\mathrm{WA}}(|y|_3) &= 0.1147^{+0.0075}_{-0.0079},\\
\alpha_S^{\mathrm{WA}}(|y|_4) &= 0.1145^{+0.0076}_{-0.0080},\\
\alpha_S^{\mathrm{WA}}(|y|_5) &= 0.1147^{+0.0072}_{-0.0077},\\
\alpha_S^{\mathrm{WA}}(|y|_6) &= 0.1155^{+0.0085}_{-0.0108},\\
\alpha_S^{\mathrm{WA}}(|y|_7) &= 0.1000^{+0.0098}_{-0.0080}.
\end{aligned}$$

Fig. 3 shows the $\alpha_S(M_Z^2)$ values obtained in the different (p_{T}; $|y|$) bins, as well as the averages obtained in the corresponding $|y|$ bins. The precision of the average in each $|y|$ bin is similar to the precision of the values obtained in the corresponding (input) p_{T} bins. This is due to the strong correlations between (and the similar size of) the uncertainties in the p_{T} bins used for the average inside a given $|y|$ bin.

Performing the combination of all the 42 (p_{T}; $|y|$) bins, one obtains

$$\alpha_S^{\mathrm{WA}} = 0.1151^{+0.0047}_{-0.0047}. \tag{8}$$

The experimental uncertainty of this average is about 30% smaller compared to the one obtained in the most precise individual $|y|$ bin (i.e. the central bin). This gain in precision is due to the rather small correlations of the systematic uncertainties, between the central and the forward region (see Fig. 2). Fig. 4 shows the global $\alpha_S(M_Z^2)$ average compared to the values obtained in individual (p_{T}; $|y|$) bins and used in the combination.

The result of this average, together with the covariance matrix of the uncertainties for the α_S values (Fig. 2(c)), have been inserted into Eq. 2, yielding a $\chi^2/\mathrm{dof} = 0.54$ (for 41 degrees of freedom). Using the same α_S^{Av} inserted in the theoretical prediction of the cross section, together with the covariance matrix of the uncertainties for the cross section values (Fig. 2(a)), yields, by comparison with the experimental cross section, a $\chi^2/\mathrm{dof} = 0.52$.

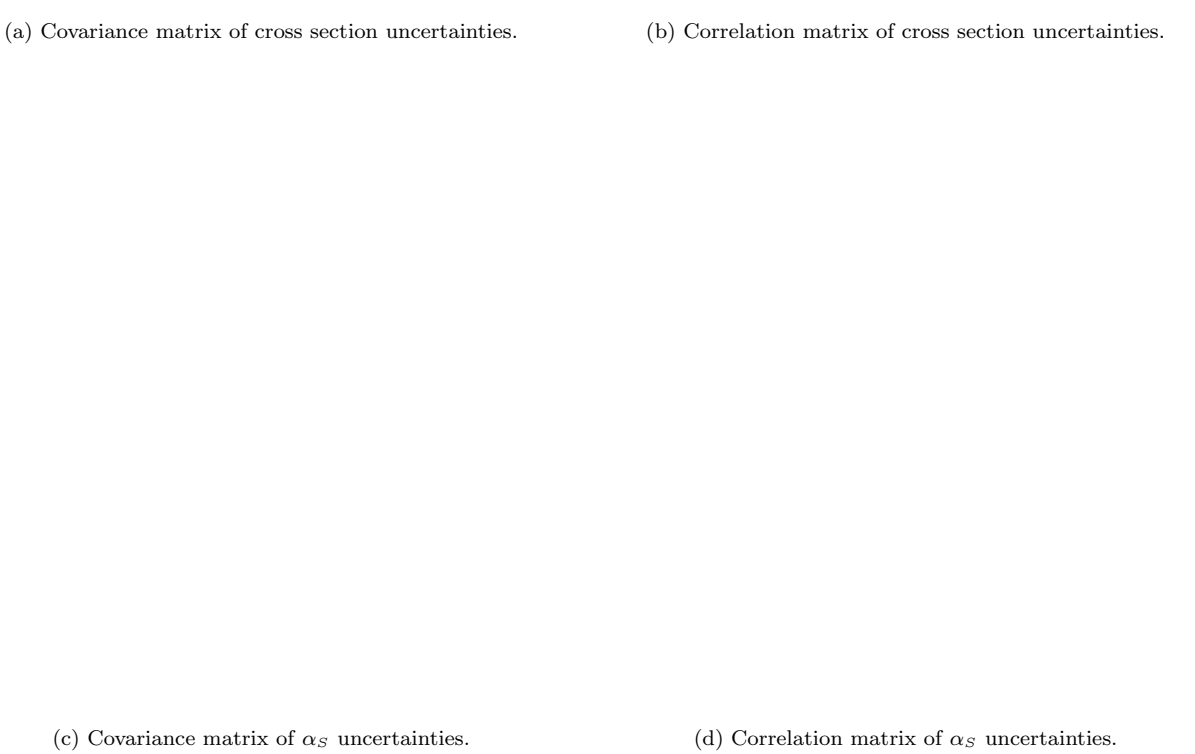

(a) Covariance matrix of cross section uncertainties.

(b) Correlation matrix of cross section uncertainties.

(c) Covariance matrix of α_S uncertainties.

(d) Correlation matrix of α_S uncertainties.

FIG. 2: Covariance (left) and correlation (right) matrices of the cross section uncertainties (top) and α_S uncertainties (bottom), in the (p_{T}; $|y|$) bins used for the final α_S average determination. The (p_{T}; $|y|$) bins are numbered as indicated in table III.

In the individual $|y|$ bins, where more than one p_{T} bin is used in the average, the χ^2/dof obtained using the corresponding weighted averages and covariance matrices are between 0.21 and 1.39. Taking into account the bin-to-bin correlations is very important for the determination of these χ^2 values. Ignoring the correlations would actually yield χ^2 values smaller by more than one order of magnitude.

An alternative averaging procedure has been tested, where the weights are obtained using only the statistical uncertainties (which exhibit rather small correlations), together with the uncorrelated components of the systematic uncertainty. However, the full information on all the uncertainties and correlations of the ATLAS measurement is used in pseudo-experiments, for the error propagation. The result obtained through this procedure is very similar to the previous ones (i.e. $0.1154^{+0.0047}_{-0.0048}$).

The results (central values and uncertainties) obtained using the simple average and these variations of the weighted average are consistent, as expected for a set

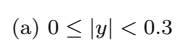

(a) $0 \leq |y| < 0.3$

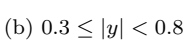

(b) $0.3 \leq |y| < 0.8$

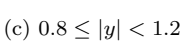

(c) $0.8 \leq |y| < 1.2$

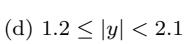

(d) $1.2 \leq |y| < 2.1$

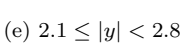

(e) $2.1 \leq |y| < 2.8$

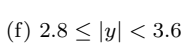

(f) $2.8 \leq |y| < 3.6$

(g) $3.6 \leq |y| < 4.4$

FIG. 3: $\alpha_S(M_Z^2)$ values (points, with asymmetric uncertainties) obtained from the ATLAS inclusive jet cross section, in all the available (p_{T}; $|y|$) bins. The different figures correspond to increasing $|y|$ values, from left to right and from top to bottom. The green band indicates the weighted averages obtained in the corresponding $|y|$ bins, and it covers only the bins which are actually used for its determination (see text).

FIG. 4: Global weighted $\alpha_S(M_Z^2)$ average (green band) together with the $\alpha_S(M_Z^2)$ values (with asymmetric uncertainties) obtained in all the $(p_{\rm T};\,|y|)$ bins used in the combination.

of inputs with similar uncertainties.

We have also tested the stability of these results when using non-Gaussian distributions for the experimental systematic uncertainties. When using log-normal distributions, the nominal values obtained from the averages in individual $|y|$ bins are very similar to the ones using Gaussian distributions, while some small changes are seen in the asymmetric uncertainties. For the result of the combination in all the $(p_{\rm T};\,|y|)$ bins, both the nominal value and the uncertainties are very similar to the ones obtained for Gaussian distributions.

D. Minimisation of a "standard" χ^2 with correlations

This procedure minimises a χ^2 with correlation (see Eq. 2), using the covariance matrix in Fig. 2(c) as input, and yields

$$\alpha_S^{\chi^2_{\rm min}} = 0.1165^{+0.0033}_{-0.0033}.$$

This result has a smaller experimental uncertainty compared to the previous averaging procedure. This is not surprising, since the Gauss-Markov theorem guarantees it to have the smallest variance, among all the weighted averages with the sum of weights equal to unity (see section IV C). However, the central value obtained here is questionable, since the weights of this average strongly rely on the exact knowledge of the bin-to-bin correlations and are not well behaved. Indeed, a large fraction (almost half) of the weights of the individual $p_{\rm T}$ bins in this average are smaller than zero. The χ^2/dof in this case is about 0.53, slightly smaller comparing to the one in the previous weighted average (as expected).

Looking at the similar averages computed in individual $|y|$ bins, they are in the range between 0.1100 and 0.1243, several of them being outside the range of the corresponding input values. This is due to the same bad behaviour of the weights, some of which are negative, while some others are larger than one. At the same time, the χ^2/dof computed in the individual $|y|$ bins (where more than one $p_{\rm T}$ bin is used in the average) are between 0.20 and 0.93.

E. Simultaneous fit of $\alpha_S(M_Z^2)$ and the luminosity, using a modified χ^2

As explained in section IV C 4, two modified χ^2 definitions (at the cross section and α_S level, respectively) were introduced, treating the luminosity uncertainty as nuisance parameter. The main goal here is to test somewhat better behaved definitions of the χ^2 with correlations.

An approximate effective dependence of $\alpha_S^{\rm Av}$ on luminosity shifts is needed in order to define the χ^2 at the α_S level, given in Eq. 6. In order to establish this dependence, a global relative shift corresponding to one standard uncertainty of the luminosity was performed, for all the cross section measurements. The first weighted average in section V C, using the total experimental uncertainty in each $(p_{\rm T};\,|y|)$ bin, was rederived. The induced variation of the weighted average yielded, within a linear approximation, the effective $\alpha_S^{\rm Av}(\beta_{\rm L})$ dependence (see Eq. 6).

Fig. 5 shows the result of the scans of the modified χ^2 values, as a function of $\alpha_S(M_Z^2)$ and the luminosity shift parameter $\beta_{\rm L}$. It shows the total χ^2 values, together with their sub-components, from the comparison between data and theory, as well as from the luminosity shift (see section IV C 4).

The partial χ^2 from the comparison between data and theory, computed at the α_S level, exhibits a degeneracy between α_S and $\beta_{\rm L}$ (see Fig. 5, top left). This is expected since, for this partial χ^2, a value obtained for a given $\alpha_S^{\rm Av}(\beta_{\rm L})$ corresponds to a combination of α_S and $\beta_{\rm L}$ values (cf. Eq. 6 which, for a fixed $\alpha_S^{\rm Av}(\beta_{\rm L})$, admits an infinity of solutions). The degeneracy is removed when adding the constraint on the luminosity shifts, which fixes the minimum of the global χ^2 at $\beta_{\rm L} = 1$. Therefore, the minimal value of the global χ^2 is equal to the minimal value of the partial χ^2 from the comparison between data and theory, and it is obtained for $\alpha_S(M_Z^2) = 0.1175$. One should recall, however, that the covariance matrix used here in the computation of the partial χ^2 from the comparison between data and theory is not complete, as the luminosity uncertainty is treated as a separate nuisance parameter. This explains the difference comparing to the result obtained from the minimisation of the "standard" global χ^2, in the previous subsection.

The degeneracy between α_S and $\beta_{\rm L}$, seen for the partial χ^2 from the comparison between data and theory, computed at the α_S level, is absent for the partial χ^2 computed at the cross section level (see Fig. 5, top right). This is due to the slightly different dependence on α_S,

FIG. 5: χ^2/dof values as a function of $\alpha_S(M_Z^2)$ and $\beta_{\rm L}$ (see text). The top figures show the contribution from the comparison between data and theory, computed at the α_S level (left) and at the cross section level (right). The center figure shows the contribution from the luminosity shifts, while the bottom figures show the total χ^2/dof, computed at the α_S level (left) and at the cross section level (right).

for the (shapes of the) theoretical calculations in the various (p_{T}; $|y|$) bins (the same effect which made Eq. 6 to be valid only as an approximation). While the above mentioned degeneracy is removed, this partial χ^2 does not allow for a strong constraint of the uncertainty on the luminosity. After adding the constraint term and minimising the total χ^2, the uncertainty on β_{L} is very similar to the input precision of the luminosity determination ($\approx 3.4\%$). The minimum of this global χ^2 is reached by a shift of the nominal luminosity which is smaller than 0.5% (much smaller than the uncertainty on the luminosity), and an $\alpha_s(M_Z^2)$ value of 0.1160.

While these two alternative χ^2 definitions still have some of the problems present for the "standard" global χ^2 (in particular, the negative weights obtained in the minimisation of the partial χ^2 from the comparison between data and theory), they show that the measurement of the inclusive jet cross section alone does not allow for an improved luminosity determination when measuring $\alpha_s(M_Z^2)$.

F. Results using a geometrical mean

Using a geometrical average (GA) for the combination, we obtain:

$$\alpha_s^{\mathrm{GA}} = 0.1149^{+0.0046}_{-0.0049}.$$

This value and its (slightly asymmetric) uncertainties are very similar to the ones obtained using the simple and the weighted averages. The same statement is true when comparing the corresponding averages in the various $|y|$ bins.

G. Conclusions on the experimental results

In the previous sections we have shown results on the $\alpha_s(M_Z^2)$ determination, using several averaging procedures. The methods using a matrix inversion in the χ^2 definition were observed to have badly behaved weights (negative or larger than one) sometimes yielding an average outside the range of the input values. Alternative averaging methods, relying on the bin-to-bin correlations for each component of the systematic uncertainties, have been proposed in the past. However, in our study, the only systematic uncertainty for which the correlations are perfectly known is the one on the ATLAS luminosity. We have shown that our study does not allow for an improvement of the luminosity determination, while performing an $\alpha_s(M_Z^2)$ measurement.

The results obtained using various weighted averages (with simple weights, or using the inverse of squared uncertainties) were shown to have (as expected) larger variances comparing to the ones using the minimisation of a χ^2 with correlations. However, these simpler weighted averages have well behaved weights, which do not rely on the exact information on the correlations, while all the information on the uncertainties and their correlations is used in the error propagation (through pseudo-experiments). In addition, these results are confirmed by the ones obtained using a geometrical average. It is for all these reasons that we choose to use the value obtained with the weights given by the inverse of the squared total uncertainties, for our nominal result.

In Fig. 4 we have shown the nominal result for $\alpha_s(M_Z^2)$, its uncertainty, and the comparison with the inputs used in the combination. The general agreement is good (except maybe for one bin from the forward region, where the theoretical prediction is more questionable), which is also confirmed by the global χ^2/dof (see Sec. V C).

The N^{3}LO RGE running based on Runge-Kuta integration, with 3-loop quark-flavour matching at the top threshold [26, 27], has been used to evolve the α_s values, from the Z scale to a given p_{T} scale. This has been done for the global average, as well as for the values obtained in the individual (p_{T}; $|y|$) bins (see Fig. 6). The reduction of the relative uncertainty on the α_s average, when performing the running from low to high p_{T} values, is also visible. In the same figure, we indicate the highest p_{T} value (145 GeV) used in the $\alpha_s(M_Z^2)$ determination, from the inclusive jet cross section, at Tevatron [28, 29]. Our combination procedure uses a p_{T} range going up to four times higher. We also use inputs from the forward region, up to $|y| = 4.4$, while the Tevatron determination is restricted to $|y| < 1.6$.

The SM running of α_s is assumed in the various PDF determinations, as well as in the theoretical calculation of the inclusive jet cross section. A possible contribution from "New Physics" would manifest by a deviation between the running of the α_s average and the individual values. This would probably be more "visible" in the figure showing the running of the inverse of α_s (see Fig. 6) [30], although one should keep in mind that the same statistical information is available in all these various ways of presenting the same result. A good agreement between our nominal fit and the 21 data points in the newly explored region, above 145 GeV, can be seen in Fig. 6 and is also shown by the corresponding partial χ^2, accounting for 8.5. The weighted average computed in the same region alone yields $0.1157^{+0.0054}_{-0.0059}$, with a χ^2/dof of 0.42 (for 20 degrees of freedom). This result is compatible with (but slightly less precise than) the nominal weighted average computed for 42 data points (Eq. 8).

As explained above, because of the limited range in the α_s scan for the theoretical prediction, not all the (p_{T}; $|y|$) bins were used in the nominal combination. This limited range in the α_s scan induces distortions in the tails of the α_s distributions for the corresponding bins. The nominal values are, however, less affected by this problem. Their combination allows for determining a systematic uncertainty due to the bins which where removed in the nominal combination, accounting for ≈ 0.0014.

Results with a similar precision are obtained using anti-k_t jets with R=0.4. The central value of the cor-

FIG. 6: Global weighted α_S average (green band) evolved to the corresponding $p_{\rm T}$ scale (left plot) and its inverse (right plot), together with the values obtained in all the ($p_{\rm T}$; $|y|$) bins used in the combination. The blue vertical line indicates the highest $p_{\rm T}$ value used in the Tevatron $\alpha_S(M_Z^2)$ determination, from the inclusive jet cross section.

responding weighted average is, however, shifted downwards with respect to our nominal result (from anti-k_t jets with R=0.6), by about 0.0060. This is expected, due to a systematic difference seen between the comparisons of the two (strongly correlated) measurements with the corresponding theoretical predictions (see section II). The study of the χ^2 scan (see section V E) applied to anti-k_t jets with R=0.4, indicates an even smaller "preferred" shift of the luminosity value, comparing to the one observed for anti-k_t jets with R=0.6. It should be pointed out that a shift in the nominal value of the luminosity (or of any other nuisance parameter which is strongly correlated between the two measurements) could not explain the observed difference anyway, as these shifts should be identical for anti-k_t jets with R=0.4 and R=0.6. The difference between the α_S determinations with the two jet sizes is treated as systematic uncertainty in our final result. This is actually our largest uncertainty and an improvement in the understanding of these differences is desirable. This improved understanding could be achieved, for example, through the measurement of the ratio between the spectra of anti-k_t jets with R=0.4 and R=0.6, and the comparison with the corresponding theoretical prediction (as given in [18]). The main challenge of this measurement is the understanding of the (strong) correlations of the systematic uncertainties of the two spectra.

H. Theoretical uncertainties

The main uncertainties on the NLO QCD prediction come from the choice of the PDF set, the uncertainties on the nominal set of PDFs and the choice of factorisation and the renormalisation scales.

In order to propagate the scale uncertainty on the cross section to the uncertainty on α_S, the theoretical cross section was recalculated with six different scale choices $(\frac{\mu_R}{\mu_R^{\rm default}}, \frac{\mu_F}{\mu_F^{\rm default}}) = \{(\frac{1}{2},1), (2,1), (1,\frac{1}{2}), (1,2), (\frac{1}{2},\frac{1}{2}), (2,2)\}$ in each ($p_{\rm T}$, $|y|$) bin. The nominal value of the measured cross section was mapped to the $\alpha_S(\mu_F,\mu_R)$ for each scale choice. The asymmetric envelope of the values $\alpha_S(\mu_F,\mu_R)$ around the one with the default scale choice is taken as the scale uncertainty on α_S. Propagating this uncertainty through our nominal averaging procedure results in a scale uncertainty on the $\alpha_S(M_Z^2)$ value of $+0.0044$ -0.0011.

For the evaluation of the uncertainty on α_S due to the choice of the PDF set, the theory prediction for the inclusive jet cross section was recalculated using MSTW 2008, NNPDF 2.1 (100) [8, 9] and HERAPDF 1.5 [10] PDF sets. For each alternative PDF set the α_S^{PDFset} was determined from the measured cross section and the recalculated theoretical one, using the procedure described in Section IV. The estimated value of the PDF choice uncertainty is $+0.0022$ -0.0015, which is the maximal difference between the α_S^{PDFset} and the central CT10 PDF one.

For the CT10 PDF the $N_p = 26$ parameters (eigenvectors) were determined. Therefore CT10 provides $2 \times N_p$ PDF uncertainty sets for positive and negative variations of each eigenvector in the N_p-dimensional parameter space [5]. The asymmetric PDF uncertainty on α_S for the CT10 PDF is given by [31]:

$$\Delta\alpha_S^+ = \sqrt{\sum_{i=1}^{N_p}\left[\max\left((\alpha_S^+)_i-(\alpha_S)_0,(\alpha_S^-)_i-(\alpha_S)_0,0\right)\right]^2}$$

$$\Delta\alpha_S^- = \sqrt{\sum_{i=1}^{N_p}\left[\max\left((\alpha_S)_0-(\alpha_S)_i^+,(\alpha_S)_0-(\alpha_S)_i^-,0\right)\right]^2},$$

where $(\alpha_S)_0$ and $(\alpha_S^\pm)_i$ are calculated using the central PDF set and $\pm$ variation of all PDF set eigenvectors, respectively. The PDF uncertainty on the average $\alpha_S(M_Z^2)$ accounts for ± 0.0010.

Finally, for the evaluation of the uncertainty on α_s due to the modelling of non-perturbative effects, the nominal value of the measured cross section was mapped to the $\alpha_S^{MC_{tune}}$ for each MC tune used to estimate the uncertainty of the non-perturbative corrections on the inclusive jet cross section. Again, the asymmetric envelope of the values $\alpha_S^{MC_{tune}}$ around the one with the default tune is taken as the uncertainty on $\alpha_s(M_Z^2)$ due to the modelling of non-perturbative effects, yielding $+0.009\ -0.0034$.

Given the fact that the theoretical systematic uncertainties from the scale choice, PDF eigenvectors, the choice of the PDF set and modelling of non-perturbative effects, are (to a good approximation) independent, the total theoretical uncertainty is equal to their quadratic sum.

VI. CONCLUSIONS

We have performed a determination of the strong coupling constant at the Z scale, using the ATLAS inclusive jet cross section data. Our final result accounts for

$$\begin{aligned}\alpha_s(M_Z^2) \;=\; & 0.1151 \pm 0.0001\ (\text{stat.}) \pm 0.0047\ (\text{exp. syst.}) \\ & \pm 0.0014\ (\text{p}_\text{T}\ \text{range}) \pm 0.0060\ (\text{jet size}) \\ & {}^{+0.0044}_{-0.0011}\ (\text{scale}) {}^{+0.0022}_{-0.0015}\ (\text{PDF choice}) \\ & \pm 0.0010\ (\text{PDF eig.}) {}^{+0.0009}_{-0.0034}\ (\text{NP corrections}),\end{aligned}$$

where the uncertainties are statistical and experimental systematic (propagated from the ATLAS data), due to the limited p_T range, due to the differences between the results obtained with the R=0.4 and R=0.6 jet sizes, due to the renormalisation and factorisation scale choice in the theoretical calculation, due to the choice of the PDF set, propagated from the PDF eigenvectors, and due to the non-perturbative corrections, respectively. Our value is in good agreement with the latest (preliminary) update of the $\alpha_s(M_Z^2)$ world average (0.1183 ± 0.0010) [32], as well as with the latest result from a hadron-hadron collider $(0.1161^{+0.0041}_{-0.0048})$ [28, 29]. Although our result is less precise, it includes for the first time the measurements of the inclusive jet cross section up to 600 GeV. The running of α_s has also been tested, in the p_T range between 45 and 600 GeV, and no evidence of a deviation from the QCD prediction has been observed.

We thank T. Carli for numerous discussions as well as a careful reading of this manuscript. We acknowledge A. Cooper-Sarkar, C. Doglioni, A. Glazov and A. Hoecker for helpful discussions. We benefited from the feedback of the ATLAS PDF forum and the ATLAS jet physics group on our study. We gratefully acknowledge ATLAS Physics Coordination and ATLAS management for fruitful discussions and continuous support.

[1] G. Aad *et al.* [ATLAS Collaboration], arXiv:1112.6297 [hep-ex].
[2] M. Cacciari, G. P. Salam and G. Soyez, JHEP **0804** (2008) 063 [arXiv:0802.1189 [hep-ph]].
[3] M. Cacciari and G. P. Salam, Phys. Lett. B **641** (2006) 57 [hep-ph/0512210].
[4] Z. Nagy, Phys. Rev. D **68** (2003) 094002 [hep-ph/0307268].
[5] H. -L. Lai *et al.*, Phys. Rev. D **82** (2010) 074024 [arXiv:1007.2241 [hep-ph]].
[6] T. Carli *et al.*, Eur. Phys. J. C **66** (2010) 503 [arXiv:0911.2985 [hep-ph]].
[7] A. D. Martin, W. J. Stirling, R. S. Thorne and G. Watt, Eur. Phys. J. C **63** (2009) 189 [arXiv:0901.0002 [hep-ph]].
[8] R. D. Ball, V. Bertone, F. Cerutti, L. Del Debbio, S. Forte, A. Guffanti, J. I. Latorre and J. Rojo *et al.*, Nucl. Phys. B **849** (2011) 296 [arXiv:1101.1300 [hep-ph]].
[9] R. D. Ball *et al.* [The NNPDF Collaboration], Nucl. Phys. B **855** (2012) 153 [arXiv:1107.2652 [hep-ph]].
[10] H1 and ZEUS Collaborations, H1prelim-10-142, ZEUS-prel-10-018.
[11] M. Dasgupta, L. Magnea and G. P. Salam, JHEP **0802** (2008) 055 [arXiv:0712.3014 [hep-ph]].
[12] M. Dasgupta and Y. Delenda, JHEP **0907** (2009) 004 [arXiv:0903.2187 [hep-ph]].
[13] ATLAS Collaboration, ATL-PHYS-PUB-2011-009.
[14] ATLAS Collaboration, ATL-PHYS-PUB-2011-008.
[15] P. Z. Skands, arXiv:0905.3418 [hep-ph].
[16] P. Z. Skands, Phys. Rev. D **82** (2010) 074018 [arXiv:1005.3457 [hep-ph]].
[17] M. Bahr *et al.*, Eur. Phys. J. C **58** (2008) 639 [arXiv:0803.0883 [hep-ph]].
[18] G. Soyez, Phys. Lett. B **698** (2011) 59 [arXiv:1101.2665 [hep-ph]].
[19] G. Aad *et al.* [Atlas Collaboration], Eur. Phys. J. C **71** (2011) 1512 [arXiv:1009.5908 [hep-ex]].
[20] G. D'Agostini, Nucl. Instrum. Meth. A **346** (1994) 306.
[21] K. Nakamura *et al.* (Particle Data Group), J. Phys. G 37, 075021 (2010), available on the PDG WWW pages (URL: http://pdg.lbl.gov/)
[22] V. Blobel, *In the Proceedings of PHYSTAT2003: Statistical Problems in Particle Physics, Astrophysics, and Cosmology, Menlo Park, California, 8-11 Sep 2003.*
[23] C. Pascaud and F. Zomer, LAL-95-05 (1995), Orsay.
[24] M. Botje, J. Phys. G G **28** (2002) 779 [hep-ph/0110123].
[25] B. List, talk at the "Alliance Workshop on Unfolding and Data Correction", DESY (2010).
[26] K. G. Chetyrkin, B. A. Kniehl and M. Steinhauser, Phys. Rev. Lett. **79** (1997) 2184 [hep-ph/9706430].
[27] G. Rodrigo, A. Pich and A. Santamaria, Phys. Lett. B **424** (1998) 367 [hep-ph/9707474].
[28] V. M. Abazov *et al.* [D0 Collaboration], Phys. Rev. D **80** (2009) 111107 [arXiv:0911.2710 [hep-ex]].
[29] D. Bandurin [for the D0 and CDF Collaboration], arXiv:1112.0051 [hep-ex].
[30] C. Quigg, *at the LHeC workshop, Divonne (2009)* and

arXiv:1202.4391 [hep-ph].
[31] J. M. Campbell, J. W. Huston and W. J. Stirling, Rept. Prog. Phys. **70** (2007) 89 [arXiv:hep-ph/0611148].
[32] S. Bethke *et al.*, Proceedings of the "Workshop on Precision Measurements of α_s", arXiv:1110.0016 [hep-ph].